JOURNAL OF NANOMATERIALS AND DEVICES
Jul-Dec 2023, VOL. 1, ISSUE 1, pp. 24-36
https://doi.org/10.61577/jnd.2023.100006

RESEAPRO JOURNALS

ORIGINAL ARTICLE

OPEN ACCESS

Chaotic forced vibration analysis of a single-walled carbon nanotube resting on elastic foundations

Ahmed Amoo Yinusa, Chibuike David Ogbonna, Victor Oluwapelumi Dada and Gbeminiyi Musibau Sobamowo

Department of Mechanical Engineering, University of Lagos, Akoka, Lagos State, Nigeria

ABSTRACT

Chaotic presence in nanotube (CNT) vibration is a potential source of imprecision and instability in nanomechanical systems. It is for this reason that the major focus of this paper is on the subject. The system's vibration model is developed using the Euler–Bernoulli beam and nonlocal theory with consideration of transverse harmonic force, thermal term, magnetic field, and Pasternak foundation influences. The equation of motion is then solved using the Galerkin decomposition method and the Differential transform method (DTM). The influences of velocity, nonlocal parameters, transverse harmonic force, and length on the nonlinear vibration of the nanotube are analyzed using the simulations contained in this paper. For the purpose of convergence and dynamic response analysis, the obtained results in this study were treated with the use of the Cosine-after treatment technique (CAT). The outcome indicates that the controlling parameters such as harmonic force, nonlocal terms, velocity and all other included terms have considerable effects on the behavior of a CNT and can be used as effective control parameters for avoiding chaos.

KEYWORDS

Chaotic forced vibration; Single-walled carbon nanotube; Elastic foundation; Nonlocal Euler-Bernoulli beam theory; Galerkin decomposition method; Differential transform method

ARTICLE HISTORY

Received 27 September 2023; Revised 19 November 2023; Accepted 26 November 2023

Introduction

Nanotechnology has become significantly relevant in our society today, hence the need to study carbon nanotubes (CNTs) because of their high frequency, brought about by their light weight and high stiffness. These peculiar properties are studied and optimized accordingly to increase their performance as it relates to nanotechnology.

Mohamed and Nazira carried out a pioneering investigation on the stability and vigorous behaviors of imperfect and perfect CNTs in pre- and post-buckling fields, as well as to introduce effects that would be insignificant in the conventional continuum proposition, such as the scale of the CNTs length, strain and stress in the micro level [1]. However, their approach was restricted to the application of Doublet mechanics (DM). Notwithstanding, the model proved effective in the design of nano-sensors, nano-actuators, and NEMS. Ebrahimi investigated the turbulent vibrations of a CNT which is supported at both ends and subjugated to a traversing force in harmonic motion [2]. The work was limited to a single-axis mechanical system with transverse harmonic force. The velocity, amplitude of traverse force, and nonlocal parameters, among other variables, were found to significantly influence the behavior of bifurcations and can act as regulatory mechanisms for preventing chaos. Farshidianfar and Soltani conducted a periodical solution for the vibration of nonlinear fluid conveying single-walled CNT [3]. The work entailed developing a model that is nonlinear for vibration of the single-walled CNT utilizing Eringen's non-local theory of elasticity. One significant limitation here is that it was solely reliant on the balance method of the nonlocal continuum thesis. Xiaolei et al. focused on the performance of a vibrational analysis of CNTs conveying fluid based on the Spectral element method of Timoshenko beam theory [4]. Their study was limited to the basis of the Timoshenko beam (nonlocal); hence it cannot be extended beyond this scope. Ansari et al. studied the Torsional vibrational analysis of CNTs [5]. The analysis of their work was based on the theory of Strain gradient and Molecular Dynamics simulations. Donald and Paulo based their research on beam oscillations on an elastic foundation (nonlinear) under recurring loads [6]. The major clampdown here is that it only focused on periodic loads while other forms were not considered. Mohammad and Sadeghi-Goughari performed research on the vibration analysis of SWCNT conveying fluid while being subjugated to only a magnetic field in the longitudinal axis (this is a constraint as other forms were not considered) [7]. It is evident from their results that in the existence of a powerful longitudinal magnetic field, the effect of nonlocal parameters and internal fluid flow on the vibratory frequencies of the single-walled CNT can be reduced to a specific degree. Yinusa et al. performed research work that dealt with the study of nonlinear stability (considering thermal-mechanical properties) and vibrational analyses of various end-shaped SWCNT conveying nano-magnetic fluid (viscous) which are enclosed in non-linear visco-elastic foundations under the magnetic field's influence [8]. Mohammad et al. conducted a buckling analysis for a double-walled CNT that is non-concentric in nature [9]. Going by their results, it was concluded that being off-center in the double-walled CNTs reduces the effects of the tube's inner boundary condition. Hossein and Milad performed research work that was based on the non-linear vibrations of multi-walled CNTs under several boundary conditions [10]. Barari et al. utilize parametrized perturbation (PPM) and

***Correspondence:** Dr. Ahmed Amoo Yinusa, Mechanical Engineering Department, University of Lagos, Nigeria, e-mail: aayinusa@unilag.edu.ng

variational iteration (VIM) methods to examine the non-linear vibration of Euler-Bernoulli beams subjected to centralized-axial loads [11]. Mohammad et al. made use of a novel shear deformation beam theory to perform the analysis of the forced vibration (damped) of the CNTs [12]. It was noted that the abating resonant effect increased as the value of the nonlocal parameter increased, thereby resulting in a rise in the nanotube's physical structure. Ahmad et al. employed the differential transformation method (DTM) in order to find the semi-analytical solutions of SI (susceptible and infected) and SIS (susceptible, infected, and susceptible) epidemic models for constant population [13]. Ganesh studied CNTs as having exceptional mechanical and electrical properties; hence, various methods have been used to thoroughly investigate their growth [14]. The properties of CNT are studied for specific conditions. Moreover, one obvious gap here is that it only shows the application of CNT to the medical and chemical industries. Suparat et al. utilized water hyacinth as a prequel to integrate multi-walled CNTs employing a simple method involving chemical vapor deposition [15]. Ravi and Deol utilized DTM to study the behavior of a SWCNT under buckling [16]. It was noted that the present method could also be applied to linear and nonlinear problems. Orynyak et al. suggested a technique for determining the amplitudes and frequencies of acoustic vibrations caused by fluid traveling in lengthy pipelines with closed branches [17]. The initial analysis of the forced vibrations of secondary steam lines caused by turbulent vortices in closed toroidal sections has been completed. Vibration stresses and velocities of pipelines were calculated using equations of fluid-pipeline interaction and compared to measurement data, while resonant amplitudes and frequencies of the vibrations were assessed. Akour studied the behavior of a non-linear beam that is simply supported and resting on the elastic foundation which is subjugated to harmonic loading [18]. The main parameters that were investigated include damping coefficient, nonlinear term's coefficient, and natural frequency. Fakhrabadi et al. examined the influence of the nonlocal elasticity theory on the electromechanical behavior of activated single-walled carbon nanotubes (SWCNTs) [19]. It was determined that nonclassical theorems like the nonlocal elasticity theory should be used to examine the mechanical and electromechanical behaviors of the nanostructures to produce more accurate results. Mohammadimehr et al. used non-local elasticity theory to build the Timoshenko model for beams to study the buckling of double-walled carbon nanotubes (DWCNTs) embedded in an elastic medium [20]. The findings demonstrated that if the small-scale effect was disregarded for long nanotubes, the critical buckling stress might be overstated using the local beam model. Wang et al. were interested in the buckling analysis of micro-rods and nano-rods based on the Timoshenko beam theory and nonlocal elasticity theory of Eringen [21]. Axially loaded rods and tubes with varying end conditions were used to develop explicit formulas for the critical buckling loads. The sensitivity of the small-scale influence on the buckling loads was also noted by comparison with the traditional beam models. Kumar et al. studied the buckling of CNTs [22]. To produce variationally consistent boundary conditions, a dynamic technique was used, taking into account both stress and strain gradient approaches. Kiani studied the vibration behavior of carbon nanotube reinforced composite (CNTRC) plates infused with layers of piezoelectric elements at the top and bottom surfaces [23]. It was demonstrated that a closed-circuit plate's fundamental frequency was always greater than one with open boundary conditions. Sears and Batra made use of molecular-mechanics simulations results of torsional and axial deformations of a SWCNT from existing papers to find shear modulus, Young's modulus, and the wall thickness of an equal tube length made of an elastic isotropic material [24]. Shen and Xiang investigated the behaviors of SWCNTs reinforced nanocomposite beams resting on a thermo-elastic foundation, including large amplitude vibration, nonlinear bending, and thermal post-buckling [25]. Consideration was given to uniformly distributed (UD) and functionally graded (FG) reinforcements for two different types of carbon nanotube-reinforced composite (CNTRC) beams. Han and Elliott addressed the elastic properties of CNT composites and went on to conduct molecular dynamics simulations to closely observe these features [26]. The potential for CNTs to improve the structural, mechanical, and electrical properties of the resulting composite led researchers to conclude that they are promising additions to polymeric materials. The simulation results were compared to the macroscopic rule-of-mixtures for composite systems, which showed that large departures from the rule-of-mixtures can happen for strong interfacial interactions. Lee and Chang provided a nonlocal analysis depicting the consequences of flow velocity on the mode shape and vibration frequency of the fluid conveying SWCNT [27]. Liang and Yong-Su considered the internal viscous fluid flow-induced vibration in a SWCNT using the method of averaging [28]. Ebrahimian et al. studied the twisting force (torsion) of nanotubes contained in an elastic medium employing DM [29]. The results were analyzed with molecular simulations, nonlocal theory numerical methods, and molecular simulations and it was found to yield a good level of agreement. Eltaher et al. offered to investigate the joint consequences of nonlocal elasticity and surface properties on vibration characteristics of nanobeams utilizing the finite element method (FED) [30]. Also, the effectiveness of the finite element method to address a complex geometry was demonstrated and can be used for the vibration analysis of SWCNTs. Fatahi-Vajari et al. investigated the vibration of SWCNTs in the axial direction based on DM employing a length scale parameter [31]. Sobamowo et al. focused their investigations on the joint effects of temperature, magnetic field, number of walls, nonlocal parameter, initial geometric imperfection, and boundary supports on the transverse vibrations (nonlinear) of CNTs resting on nonlinear and linear elastic foundations [32]. The findings of this study were targeted to aid in the design of multi-walled CNTs in a thermal and magnetic environment for diverse electrical, structural, biological, and mechanical applications. Yinusa et al. scrutinized the nanofluid flow through MWCNT under both perfect and imperfect fence boundary conditions [33]. The findings of this study were expected to improve the design of nanomechanical CNT-based devices that carry fluid under various conditions. Gangoli et al., employing the finite element approach, suggested to investigate the coupled impacts of surface features and nonlocal elasticity on nanobeam vibration characteristics [34]. Furthermore, the ability of the finite element method to handle a complex geometry was demonstrated. This method can be applied to the free vibration analysis of SWCNTs. Torres-Dias et al. established that the Iodine chains were absorbed not in the center cavity but between the concentric graphene shells in highly crystalline

https://doi.org/10.61577/jnd.2023.100006

arc-discharge MWCNTs [35]. These findings were unique to catalyst-free procedures since catalytic processes employ low/moderate temperatures, but they apply to all geometrically inclined carbon structures developed at high temperatures.

Model Formulation

In Figure 1, a schematic representation of the nanotube model excited by a traverse load P(t) is shown. E is Young's modulus of elasticity, tb is the thickness, and L is the length. The ensuing assumptions are established in order to examine the system (Figure 2):

(a) P(t) travels with constant velocity vp along the x-direction.
(b) P(t) travels at 90 degrees to the x-direction.
(c) The SWCNT is simple-supported.
(d) The inertia influence of P(t) is neglected.
(e) CNT's lateral displacement and velocity are both set to zero for the initial condition.
(f) It is assumed that the material is homogeneous and isotropic.

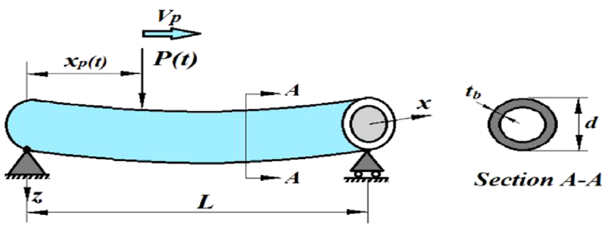

Figure 1. SWCNT's schematic under traverse loading [2].

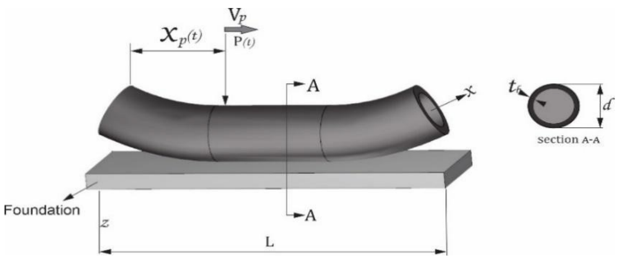

Figure 2. Re-modelling SWCNT's schematic under traverse loading on a foundation.

In accordance with Eringen's theory of nonlocal elasticity. The following is an expression for nonlocal elasticity theory:

$$(1-(e_0a)^2\nabla^2)\sigma = \tau \quad (1)$$

The stress model is expressed as follows;

$$\sigma_{xx} - (e_0a)^2\frac{\partial^2\sigma_{xx}}{\partial x^2} = E\varepsilon_{xx} \quad (2)$$

Employing the Euler-Bernoulli beam theory.

$$\frac{\partial^2 M}{\partial x^2} + p = \rho A\frac{\partial^2 w}{\partial t^2} + K_1 w + K_2 w^3 \quad (3)$$

Where, p is the transverse loading, ρ is the beam's density, A is the beam's area, w denotes the beam's transverse displacement, t represents time, and M denotes moment. Also, and are the Winkler-like elastic foundation coefficient, while the cube was introduced to make the equation non-linear. Expressing M and strain ε_xx as

$$M = \int z\sigma_{xx}dA \quad (4)$$

$$\varepsilon_{xx} = -z\frac{\partial^2 w}{\partial x^2} \quad (5)$$

Multiplying equation (2) by zdA and integrating, we have;

$$\int_A z\sigma_{xx}dA - (e_0a)^2\frac{\partial^2}{\partial x^2}\int_A z\sigma_{xx}dA = \int_A E(\varepsilon_{xx})zdA \quad (6)$$

Substituting equations (4) and (5) into equation (6), we have;

$$M - (e_0a)^2\frac{\partial^2 M}{\partial x^2} = \int_A E(-z\frac{\partial^2 w}{\partial x^2})zdA \quad (7)$$

Simplifying equation (7), we have;

$$M - (e_0a)^2\frac{\partial^2 M}{\partial x^2} = -EI\frac{\partial^2 w}{\partial x^2} \quad (8)$$

where I=∫ z^2 dA denotes the inertia.

Making necessary substitution, the governing equation is obtained as;

$$EI\frac{\partial^4 w(x,t)}{\partial x^4} + \rho A\frac{\partial^2}{\partial t^2}\left[w(x,t) - (e_0a)^2\frac{\partial^2 w(x,t)}{\partial x^2}\right] + K_1\left[w(x,t) - (e_0a)^2\frac{\partial^2 w(x,t)}{\partial x^2}\right] +$$

$$K_2\left[w^3(x,t) - (e_0a)^2\frac{\partial^2 w^3(x,t)}{\partial x^2}\right] = p(x,t) - (e_0a)^2\frac{\partial^2 p(x,t)}{\partial x^2} \quad (9)$$

Similarly, p(x,t) is represented as;

$$p(x,t) = P(t).\delta(x - x_p) \quad (10a)$$

Where, $p(t) = P_0 \, sin \, sin \, \Omega t$ (10b)

Substituting equations (10a) and (10b) into equation (9), and re-arranging, we have:

$$EI\frac{\partial^4 w(x,t)}{\partial x^4} + \rho A\frac{\partial^2}{\partial t^2}\left[w(x,t) - (e_0a)^2\frac{\partial^2 w(x,t)}{\partial x^2}\right] + K_1\left[w(x,t) - (e_0a)^2\frac{\partial^2 w(x,t)}{\partial x^2}\right] + \quad (11)$$

$$K_2\left[w^3(x,t) - (e_0a)^2\frac{\partial^2 w^3(x,t)}{\partial x^2}\right] - \left[(p_0\sin\Omega t).\delta(x-x_p) - (e_0a)^2\frac{\partial^2\left[(p_0\sin\Omega t).\delta(x-x_p)\right]}{\partial x^2}\right] = 0$$

Introducing some more terms to the general equation:

» Magnetic field term $= -\eta B_o^2 A\frac{\partial^2 w}{\partial x^2}$

» Thermal term $= -\frac{EI}{1-2\upsilon}\alpha\Delta T\frac{\partial^2 w}{\partial x^2}$

» Pasternak foundation term $= K_p\frac{\partial^2 w}{\partial x^2}$

Substituting these terms into equation (11) with their respective nano terms yields equation (12):

Galerkin's method

The Galerkin approach is thus utilized in transforming the partial differential equation (PDE) of equation (12) into ODE.

Thus, nanotube deflection may be represented as a product of the eigenfunctions $\Phi(x)$ and generalized coordinates $q(t)$. This is demonstrated in equation (13)

$$w(x,t) = \Phi(x).q(t) \quad (13)$$

Steps to carry-out the Galerkin's approach

1. Insert equation (13) into equation (12)
2. Multiply both sides by the eigenfunction $\Phi(x)$
3. Integrate the obtained equation over the interval $(0, L)$

Let $R_i(x,t)$ be equal to the governing equation (12)

Applying the stepwise approach of Galerkin's method yields:

$$\int_0^L R_i(x,t)\Phi(x)dx = 0 \quad (14)$$

Substituting $R_i(x,t)$ and expanding gives:

https://doi.org/10.61577/jnd.2023.100006

$$\int_0^L \left[\begin{array}{l} EI\dfrac{\partial^4 w(x,t)}{\partial x^4} + \rho A\dfrac{\partial^2}{\partial t^2}\left[w(x,t)-(e_0a)^2\dfrac{\partial^2 w(x,t)}{\partial x^2}\right] + K_1\left[w(x,t)-(e_0a)^2\dfrac{\partial^2 w(x,t)}{\partial x^2}\right] \\ +K_2\left[w^3(x,t)-(e_0a)^2\dfrac{\partial^2\left(w^3(x,t)\right)}{\partial x^2}\right] - \eta B_o^2 A\dfrac{\partial^2}{\partial x^2}\left[w(x,t)-(e_0a)^2\dfrac{\partial^2 w(x,t)}{\partial x^2}\right] \\ -\dfrac{EI}{1-2\upsilon}\alpha\Delta T\dfrac{\partial^2}{\partial x^2}\left[w(x,t)-(e_0a)^2\dfrac{\partial^2 w(x,t)}{\partial x^2}\right] \\ +K_p\dfrac{\partial^2}{\partial x^2}\left[w(x,t)-(e_0a)^2\dfrac{\partial^2 w(x,t)}{\partial x^2}\right] \\ -\left[(p_0\sin\Omega t).\delta(x-x_p)-(e_0a)^2\dfrac{\partial^2\left[(p_0\sin\Omega t).\delta(x-x_p)\right]}{\partial x^2}\right]=0 \end{array}\right]\Phi(x)dx=0 \tag{15}$$

Therefore, we now perform a term-by-term conversion of the above equation to turn it into an ODE.

1st Term:

$$\int_0^L\left[EI\frac{\partial^4 w(x,t)}{\partial x^4}+K_p\frac{\partial^2}{\partial x^2}\left[w(x,t)-(e_0a)^2\frac{\partial^2 w(x,t)}{\partial x^2}\right]\right]\Phi(x)dx$$

$$\int_0^L\left[EI\frac{\partial^4(\Phi(x).q(t))}{\partial x^4}+K_p\left[\frac{\partial^2(\Phi(x).q(t))}{\partial x^2}-(e_0a)^2\frac{\partial^4(\Phi(x).q(t))}{\partial x^4}\right]\right]\Phi(x)dx$$

$$=\left[\int_0^L EI\Phi(x)\frac{\partial^4\Phi(x)}{\partial x^4}dx\right]q(t)+\left[\int_0^L K_p\Phi(x)\left[\frac{\partial^2\Phi(x)}{\partial x^2}-(e_0a)^2\frac{\partial^4\Phi(x)}{\partial x^4}\right]dx\right]q(t)$$

$$=\left[\int_0^L\left[EI\Phi(x)\frac{\partial^4\Phi(x)}{\partial x^4}+K_p\Phi(x)\left[\frac{\partial^2\Phi(x)}{\partial x^2}-(e_0a)^2\frac{\partial^4\Phi(x)}{\partial x^4}\right]\right]dx\right]q(t) \tag{16}$$

2nd Term:

$$\int_0^L\rho A\frac{\partial^2}{\partial t^2}\left[w(x,t)-(e_0a)^2\frac{\partial^2 w(x,t)}{\partial x^2}\right]\Phi(x)dx$$

$$=\int_0^L\rho A\left[\frac{\partial^2\Phi(x).q(t)}{\partial t^2}\Phi(x)-(e_0a)^2\frac{\partial^4\Phi(x).q(t)}{\partial x^2\partial t^2}\Phi(x)\right]dx$$

$$=\left[\int_0^L\rho A\Phi(x)\left[\Phi(x)-(e_0a)^2\frac{\partial^2\Phi(x)}{\partial x^2}\right]dx\right]\ddot{q}(t) \tag{17}$$

3rd Term:

$$\int_0^L\left[K_1\left[w(x,t)-(e_0a)^2\frac{\partial^2 w(x,t)}{\partial x^2}\right]-\left(\eta B_o^2A+\frac{EI}{1-2\upsilon}\alpha\Delta T\right)\frac{\partial^2}{\partial x^2}\left[w(x,t)-(e_0a)^2\frac{\partial^2 w(x,t)}{\partial x^2}\right]\right]\Phi(x)dx$$

$$=\int_0^L\left[\begin{array}{l} K_1\left[\Phi^2(x)q(t)-(e_0a)^2\Phi(x)\dfrac{\partial^2\Phi(x)}{\partial x^2}q(t)\right] \\ -\left(\eta B_o^2A+\dfrac{EI}{1-2\upsilon}\alpha\Delta T\right)\left[\dfrac{\partial^2\Phi(x).q(t)}{\partial x^2}\Phi(x)-(e_0a)^2\dfrac{\partial^4\Phi(x).q(t)}{\partial x^4}\Phi(x)\right]\end{array}\right]dx$$

$$=\left[\int_0^L\left[\begin{array}{l} K_1\Phi(x)\left[\Phi(x)-(e_0a)^2\dfrac{\partial^2\Phi(x)}{\partial x^2}\right] \\ -\left(\eta B_o^2A+\dfrac{EI}{1-2\upsilon}\alpha\Delta T\right)\Phi(x)\left[\dfrac{\partial^2\Phi(x)}{\partial x^2}-(e_0a)^2\dfrac{\partial^4\Phi(x)}{\partial x^4}\right]\end{array}\right]dx\right]q(t) \tag{18}$$

4th Term:

$$\int_0^L K_2\left[w^3(x,t)-(e_0a)^2\frac{\partial^2 w^3(x,t)}{\partial x^2}\right]\Phi(x)dx$$

$$=\int_0^L K_2\left[w^3(x,t)-(e_0a)^2\left[6w(x,t)\left[\frac{\partial w(x,t)}{\partial x}\right]^2+3(w(x,t))^2\left[\frac{\partial^2 w(x,t)}{\partial x^2}\right]\right]\right]\Phi(x)dx$$

$$=\int_0^L K_2\left[\Phi^4(x)q^3(t)-(e_0a)^2 3\Phi^2(x)q^3(t)\left[2\left(\frac{\partial\Phi(x)}{\partial x}\right)^2+\Phi(x)\frac{\partial^2\Phi(x)}{\partial x^2}\right]\right]dx$$

$$=\left[\int_0^L K_2\Phi^2(x)\left[\Phi^2(x)-3(e_0a)^2\left[2\left(\frac{\partial\Phi(x)}{\partial x}\right)^2+\Phi(x)\frac{\partial^2\Phi(x)}{\partial x^2}\right]\right]dx\right]q^3(t) \tag{19}$$

5th Term:

$$-\int_0^L\left[(p_0\sin\Omega t).\delta(x-x_p)-(e_0a)^2\frac{\partial^2\left[(p_0\sin\Omega t).\delta(x-x_p)\right]}{\partial x^2}\right]\Phi(x)dx$$

$$=-\int_0^L(p_0\sin\Omega t)\left[\Phi(x).\delta(x-x_p)-(e_0a)^2\frac{\partial^2(\Phi(x).\delta(x-x_p))}{\partial x^2}\right]dx \tag{20}$$

Rearranging and grouping like terms, the Galerkin method yields the following Duffing equation:

$$M\ddot{q}(t)+Cq(t)+Vq^3(t)+J=0 \tag{21}$$

Where:

$$M=\int_0^L\rho A\Phi(x)\left[\Phi(x)-(e_0a)^2\frac{\partial^2\Phi(x)}{\partial x^2}\right]dx$$

$$C=\int_0^L\left[\begin{array}{l}\left[EI\Phi(x)\dfrac{\partial^4\Phi(x)}{\partial x^4}+K_p\Phi(x)\left[\dfrac{\partial^2\Phi(x)}{\partial x^2}-(e_0a)^2\dfrac{\partial^4\Phi(x)}{\partial x^4}\right]\right] \\ +\left[K_1\Phi(x)\left[\Phi(x)-(e_0a)^2\dfrac{\partial^2\Phi(x)}{\partial x^2}\right]-\left(\eta B_o^2A+\dfrac{EI}{1-2\upsilon}\alpha\Delta T\right)\Phi(x)\left[\dfrac{\partial^2\Phi(x)}{\partial x^2}-(e_0a)^2\dfrac{\partial^4\Phi(x)}{\partial x^4}\right]\right]\end{array}\right]$$

$$=\int_0^L\Phi(x)\left[\begin{array}{l} EI\dfrac{\partial^4\Phi(x)}{\partial x^4}+\left[\dfrac{\partial^2\Phi(x)}{\partial x^2}-(e_0a)^2\dfrac{\partial^4\Phi(x)}{\partial x^4}\right]\left[K_p-\left(\eta B_o^2A+\dfrac{EI}{1-2\upsilon}\alpha\Delta T\right)\right] \\ +K_1\left[\Phi(x)-(e_0a)^2\dfrac{\partial^2\Phi(x)}{\partial x^2}\right]\end{array}\right]dx$$

$$V=\left[\int_0^L K_2\Phi^2(x)\left[\Phi^2(x)-3(e_0a)^2\left[2\left(\frac{\partial\Phi(x)}{\partial x}\right)^2+\Phi(x)\frac{\partial^2\Phi(x)}{\partial x^2}\right]\right]dx\right]$$

$$J=-\int_0^L(p_0\sin\Omega t)\left[\Phi(x).\delta(x-x_p)-(e_0a)^2\frac{\partial^2(\Phi(x).\delta(x-x_p))}{\partial x^2}\right]dx$$

Equation (21) is the desired system of ODE from Galerkin's decomposition of the PDEs which will be solved using DTM.

Solution of the Model using Differential Transformation Method (DTM)

Applying DTM, equation (19) becomes:

$$M(k+1)(k+2)q[k+2]+Cq[k]+V\sum_{p=0}^{k}\sum_{l=0}^{p}q[l]\cdot q[p-l]\cdot q[k-p]+J\delta(k)=0 \tag{22}$$

$$\therefore q[k+2]=\frac{-J\delta(k)-V\sum_{p=0}^{k}\sum_{l=0}^{p}q[l]\cdot q[p-l]\cdot q[k-p]-Cq[k]}{M(k+1)(k+2)} \tag{23}$$

https://doi.org/10.61577/jnd.2023.100006

When k=0, i.e., $q[k+2]=q[0+2]=q[2]$

$$q[2]=-\frac{J\delta(0)+V(q[0])^3+Cq[0]}{2M} \tag{24}$$

$q[0]$ and $q[1]$ can be gotten from the initial boundary conditions:
Let:
initial displacement be $q=\lambda$
initial velocity, $\dot{q}=v_1=0$

$$\therefore q=q[k]=q[0]=\lambda \text{ at k=0} \tag{25}$$

Also,

$$\dot{q}=(k+1)q[k+1]=0$$

$$\therefore q[1]=0 \tag{26}$$

$$\delta=k\rightarrow piecewise(k=0,1,k\neq 0,0)$$

$$\therefore \delta[0]=1 \tag{27}$$

Hence, $q[2]$ becomes:

$$q_2=-\frac{V\lambda^3+C\lambda+J}{2M} \tag{28}$$

Iterating for $k=1,2,3,4,5$ and 6 gives the following value for $q[k]$

$$q_3=0 \tag{29}$$

$$q_4=-\frac{-\frac{3V\lambda^2(V\lambda^3+C\lambda+J)}{2M}-\frac{C(V\lambda^3+C\lambda+J)}{2M}}{12M} \tag{30}$$

$$q_5=0 \tag{31}$$

$$q_6=-\frac{V\left(-\frac{\lambda^2\left(-\frac{3V\lambda^2(V\lambda^3+C\lambda+J)}{2M}-\frac{C(V\lambda^3+C\lambda+J)}{2M}\right)}{4M}+\frac{3\lambda(V\lambda^3+C\lambda+J)^2}{4M^2}\right)-\frac{C\left(-\frac{3V\lambda^2(V\lambda^3+C\lambda+J)}{2M}-\frac{C(V\lambda^3+C\lambda+J)}{2M}\right)}{12M}}{30M} \tag{32}$$

$$q_7=0 \tag{33}$$

$$q_8=-\frac{1}{56M}\left(V\left(-\frac{\lambda^2\left(V\left(-\frac{\lambda^2\left(-\frac{3V\lambda^2(V\lambda^3+C\lambda+J)}{2M}-\frac{C(V\lambda^3+C\lambda+J)}{2M}\right)}{4M}+\frac{3\lambda(V\lambda^3+C\lambda+J)^2}{4M^2}\right)-\frac{C\left(-\frac{3V\lambda^2(V\lambda^3+C\lambda+J)}{2M}-\frac{C(V\lambda^3+C\lambda+J)}{2M}\right)}{12M}\right)}{10M}+\frac{\lambda(V\lambda^3+C\lambda+J)\left(-\frac{3V\lambda^2(V\lambda^3+C\lambda+J)}{2M}-\frac{C(V\lambda^3+C\lambda+J)}{2M}\right)}{4M^2}-\frac{(V\lambda^3+C\lambda+J)^3}{8M^3}\right)-\frac{C\left(V\left(-\frac{\lambda^2\left(-\frac{3V\lambda^2(V\lambda^3+C\lambda+J)}{2M}-\frac{C(V\lambda^3+C\lambda+J)}{2M}\right)}{4M}+\frac{3\lambda(V\lambda^3+C\lambda+J)^2}{4M^2}\right)-\frac{C\left(-\frac{3V\lambda^2(V\lambda^3+C\lambda+J)}{2M}-\frac{C(V\lambda^3+C\lambda+J)}{2M}\right)}{12M}\right)}{30M}\right) \tag{34}$$

The expression for the lateral displacement of the CNT as a function of the time passed is given as:

$$w[t]=\sum_{i=0}^{k}q[i]t^i=q_6t^6+q_5t^5+q_4t^4+q_3t^3+q_2t^2+q_1t+q_0 \tag{35}$$

Substituting the values for to yields:

$$w[t]=\lambda-\frac{(V\lambda^3+C\lambda+J)t^2}{2M}-\frac{\left(-\frac{3V\lambda^2(V\lambda^3+C\lambda+J)}{2M}-\frac{C(V\lambda^3+C\lambda+J)}{2M}\right)t^4}{12M}-\frac{\left(V\left(-\frac{\lambda^2\left(-\frac{3V\lambda^2(V\lambda^3+C\lambda+J)}{2M}-\frac{C(V\lambda^3+C\lambda+J)}{2M}\right)}{4M}+\frac{3\lambda(V\lambda^3+C\lambda+J)^2}{4M^2}\right)-\frac{C\left(-\frac{3V\lambda^2(V\lambda^3+C\lambda+J)}{2M}-\frac{C(V\lambda^3+C\lambda+J)}{2M}\right)}{12M}\right)t^6}{30M} \tag{36}$$

The above is the DTM solution of the Duffing equation. The displacement equation, $w(x,t)$, which is our major focus is calculated thus:
Recall, $w(x,t)=\Phi(x).q(t)$
Substituting the value of $q(t)$ in the above yields:

$$w(x,t)=\left[\lambda-\frac{(V\lambda^3+C\lambda+J)t^2}{2M}-\frac{\left(-\frac{3V\lambda^2(V\lambda^3+C\lambda+J)}{2M}-\frac{C(V\lambda^3+C\lambda+J)}{2M}\right)t^4}{12M}-\frac{\left(V\left(-\frac{\lambda^2\left(-\frac{3V\lambda^2(V\lambda^3+C\lambda+J)}{2M}-\frac{C(V\lambda^3+C\lambda+J)}{2M}\right)}{4M}+\frac{3\lambda(V\lambda^3+C\lambda+J)^2}{4M^2}\right)-\frac{C\left(-\frac{3V\lambda^2(V\lambda^3+C\lambda+J)}{2M}-\frac{C(V\lambda^3+C\lambda+J)}{2M}\right)}{12M}\right)t^6}{30M}\right]\Phi(x) \tag{37}$$

The displacement equation is then solved for different conditions of CNT.
For Simply supported:

$$\Phi(x)=\sin\left(\frac{n\pi}{L}x\right) \tag{38}$$

The initial and boundary conditions

In this work, we shall commence with simply supported.

$$\Phi(x)=\sin\left(\frac{n\pi}{L}x\right)$$

The initial and the boundary conditions are:

$$w(x,0)=a,\dot{w}(x,0)=0$$

$$w(0,t)=w'(0,t)=0,w(L,t)=w''(L,t)=0$$

Hence, for simply supported, the following constants from above becomes:

$$M=L\rho A\sin\left[\frac{\pi nx}{L}\right]\left[\frac{\sin\pi nx}{L}\right] \tag{39}$$

$$C=L\sin\left[\frac{\pi nx}{L}\right]K_1\left[\sin\left[\frac{\pi nx}{L}\right]\right] \tag{40}$$

$$V=LK_2\sin\left[\frac{\pi nx}{L}\right]\left[\sin\left[\frac{\pi nx}{L}\right]^3\right] \tag{41}$$

Substituting the values of the involved parameters, and expanding equations (39), (40), and (41):

$$M=-\frac{(\cos(\frac{n\pi h}{L})\sin(\frac{n\pi h}{L})L-n\pi h)\rho A}{2n\pi}-\frac{(\cos(\frac{n\pi h}{L})\sin(\frac{n\pi h}{L})L-n\pi h)n\pi\rho A(\grave{o})^2}{2L^2} \tag{42}$$

$$\begin{aligned}C=&-\frac{(\cos(\frac{n\pi h}{L})\sin(\frac{n\pi h}{L})L-n\pi h)n^3\pi^3EI}{2L^4}+\frac{(\cos(\frac{n\pi h}{L})\sin(\frac{n\pi h}{L})L-n\pi h)n\pi K_p}{2L^2}\\&-\frac{n\pi\eta(B_0)^2A\phi(\cos(\frac{n\pi h}{L})-1)}{L}+\frac{(\cos(\frac{n\pi h}{L})\sin(\frac{n\pi h}{L})L-n\pi h)n\pi EI\alpha(\Delta T)}{2(-1+2\upsilon)L^2}\\&+\frac{(\cos(\frac{n\pi h}{L})\sin(\frac{n\pi h}{L})L-n\pi h)n^3\pi^3\grave{o}(K_p)^2}{2L^4}-\frac{(\cos(\frac{n\pi h}{L})\sin(\frac{n\pi h}{L})L-n\pi h)n^3\pi^3\eta(B_0)^2A(\grave{o})^2}{2L^4}\\&+\frac{(\cos(\frac{n\pi h}{L})\sin(\frac{n\pi h}{L})L-n\pi h)n^3\pi^3\grave{o}^2EI\alpha(\Delta T)}{2(-1+2\upsilon)L^4}-\frac{(\cos(\frac{n\pi h}{L})\sin(\frac{n\pi h}{L})L-n\pi h)K_1^2}{2n\pi}\\&-\frac{(\cos(\frac{n\pi h}{L})\sin(\frac{n\pi h}{L})L-n\pi h)n\pi K_1(\grave{o})^2}{2L^2}\end{aligned} \tag{43}$$

https://doi.org/10.61577/jnd.2023.100006

RESEAPRO JOURNALS

$$V=-\frac{(2L\cos(\frac{n\pi h}{L})\sin(\frac{n\pi h}{L})^3+3\cos(\frac{n\pi h}{L})\sin(\frac{n\pi h}{L})L-3n\pi h)K_2}{8n\pi}-3\sin(\frac{n\pi h}{L})^4 \grave{o}(K_2)^2$$

$$-\frac{(2L\cos(\frac{n\pi h}{L})\sin(\frac{n\pi h}{L})^3+3\cos(\frac{n\pi h}{L})\sin(\frac{n\pi h}{L})L-3n\pi h)n\pi K_2(\grave{o})^2}{8L^2} \quad (44)$$

Cosine- after treatment technique (CAT technique)

This is used for a DTM transformation of a dynamic equation with even power. Consider a series which is truncated in N terms as follows:

$$\varphi(t)=\sum_{j=1}^{n}\xi_j\cos(\chi_j t) \quad (45)$$

Then using Fourier Series expansion, it becomes:

$$\varphi(t)=\sum_{j=1}^{n}\xi_j-(\sum_{j=1}^{n}\xi_j\chi_j^2)\frac{t^2}{2!}+(\sum_{j=1}^{n}\xi_j\chi_j^4)\frac{t^4}{4!}-(\sum_{j=1}^{n}\xi_j\chi_j^6)\frac{t^6}{6!}+(\sum_{j=1}^{n}\xi_j\chi_j^7)\frac{t^7}{7!}-(\sum_{j=1}^{n}\xi_j\chi_j^8)\frac{t^8}{8!}+\ldots \quad (46)$$

Comparing coefficients with Eq. (35):

$$t^0:\sum_{j=1}^{n}\xi_j=q_0$$

$$t^2:\sum_{j=1}^{n}\xi_j\chi_j^2=-2!q_2$$

$$t^4:\sum_{j=1}^{n}\xi_j\chi_j^4=4!q_4$$

$$t^6:\sum_{j=1}^{n}\xi_j\chi_j^6=-6!q_6 \quad (47)$$

An approximation of the expression in the form of a COS function is given in place of these terms. The objective is to have a function with two terms of the cosine function. This results in:

$$\varphi(t)=\sum_{j=1}^{n}\xi_j\cos(\chi_j t)=\xi_1\cdot\cos(\chi_1 t)+\xi_2\cdot\cos(\chi_2 t) \quad (48)$$

Applying the technique yields:

$$\xi_1+\xi_2=q_0$$
$$\xi_1\chi_1^2+\xi_2\chi_2^2=-2!q_2$$
$$\xi_1\chi_1^4+\xi_2\chi_2^4=4!q_4$$
$$\xi_1\chi_1^6+\xi_2\chi_2^6=-6!q_6$$

The four unknowns $\xi_1,\xi_2,\chi_1,\chi_2$ were found by solving the following system of non-linear algebraic equations numerically.

The set of values that satisfy the condition of the CAT can now be concisely written, resulting in an approximate periodic solution:

Mode n=1

$$\varphi(t)=\sum_{j=1}^{n}\xi_j\cos(\chi_j t)=2.124218836\times10^{-19}\cosh(3.030695308\times10^{21}t)+3.499999998\times10^{-10}\cosh(8.666149633\times10^{21}t)$$

Mode n=2

$$\varphi(t)=\sum_{j=1}^{n}\xi_j\cos(\chi_j t)=3.500000000\times10^{-10}\cosh(1.935842168\times10^{22}t)-1.558606599\times10^{-20}\cosh(3.072220979\times10^{22}t)$$

Mode n=3

$$\varphi(t)=\sum_{j=1}^{n}\xi_j\cos(\chi_j t)=1.609445896\times10^{-10}\cos(2.219489392\times10^{22}t)+1.890554104\times10^{-10}\cosh(3.336377497\times10^{22}t)$$

Eliminating the imaginary aspect (I) and solving in terms of cosine only, we have:

Mode n=1

$$\varphi(t)=\sum_{j=1}^{n}\xi_j\cos(\chi_j t)=2.124218836\times10^{-19}\cos(3.030695308\times10^{21}t)+3.499999998\times10^{-10}\cos(8.666149633\times10^{21}t)$$

Mode n=2

$$\varphi(t)=\sum_{j=1}^{n}\xi_j\cos(\chi_j t)=3.500000000\times10^{-10}\cos(1.935842168\times10^{22}t)-1.558606599\times10^{-20}\cos(3.072220979\times10^{22}t)$$

Mode n=3

$$\varphi(t)=\sum_{j=1}^{n}\xi_j\cos(\chi_j t)=1.609445896\times10^{-10}\cos(2.219489392\times10^{22}t)+1.890554104\times10^{-10}\cos(3.336377497\times10^{22}t)$$

Fundamental frequency, velocity of lateral displacement and critical velocity

Recall the duffing equation:

$$M\ddot{q}(t)+Cq(t)+Vq^3(t)+J=0$$

Re-writing this equation with reference to frequency, , also known as the fundamental frequency, we have:

$$\ddot{q}(t)+\omega^2q(t)=\frac{J}{\rho\cdot A\cdot(1+(e_oa)^2(\frac{\pi}{L})^2)}$$

Where:

$$\omega=\sqrt{\frac{EI(\frac{\pi}{L})^4}{\rho\cdot A\cdot(1+(e_oa)^2(\frac{\pi}{L})^2)}}$$

$$q=\frac{\cos(\omega t)}{10}$$

$$v=-\frac{\omega\sin(\omega t)}{10}$$

The velocity of the lateral displacement of the tube is given by v. Also, we shall be introducing a parameter for the critical velocity, v_{cr}, which represents the velocity of the traversing harmonic force.

$$v_{cr}=\frac{\omega L}{\pi}$$

Results and Discussion

This section presents the simulation of the results of the analysis using MATLAB. For the purpose of obtaining physical significance, a list of actual process values used and assumed for various parameters in the analysis are;

Mass density of CNT, $\rho=2300$ kg/m3

Diameter of CNT, d=1 nm = 1×10^{-9} m

Area of CNT, A=1.96×10^{-19} m2

Length of CNT, L=40 nm = 40×10^{-9} m

Non-local parameter, ò=$e_0a=0.058$ nm

Young's Modulus, $E=1$ TPa = 1×10^{12} Pa

Moment of Inertia, $I=7.23\times10^{-23}$ Kg·m2

Pasternak foundation coefficient, $K_p=7.226\times10^{-8}$

Winkler-elastic coefficient, $K_1=K_2=7.226\times10^{-8}$

Magnetic field strength, $B_0=40\times10^{-6}$ T

Vacuum permeability, η=1.26×10^{-6} Tm/A

Poisson's ratio, υ=0.2

Thermal expansion coefficient, $\alpha=10^{-6}$ K-1

Temperature change (assumed), ΔT=2K

Applied traversal harmonic force, $J=0.5\times10^{-3}$ N

Initial displacement, $\lambda=0.35\times10^{-9}$ m and Upper limit for the integral, $h=1$

Dynamic response analysis

The dynamic response of the nanotube deals with the relationship that exists between the lateral displacement of the CNT and across a set of time intervals for the different mode shapes. This dynamic response will be analyzed under different controlling parameters.

https://doi.org/10.61577/jnd.2023.100006

RESEAPRO JOURNALS

Dynamic response without considering the after-treatment technique (Figures 3-6)

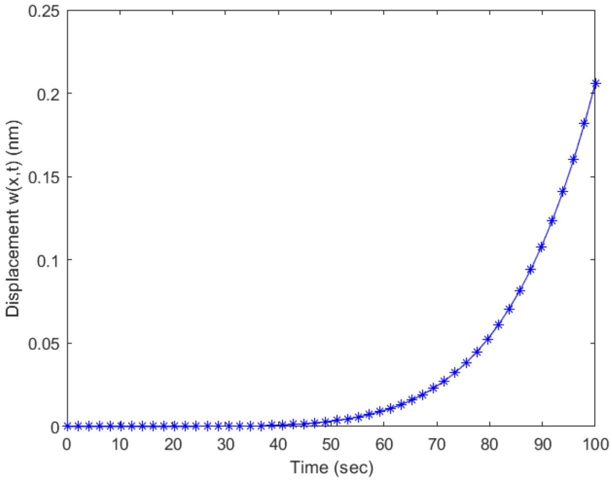

Figure 3. Response of the tube at mode 1 (n=1).

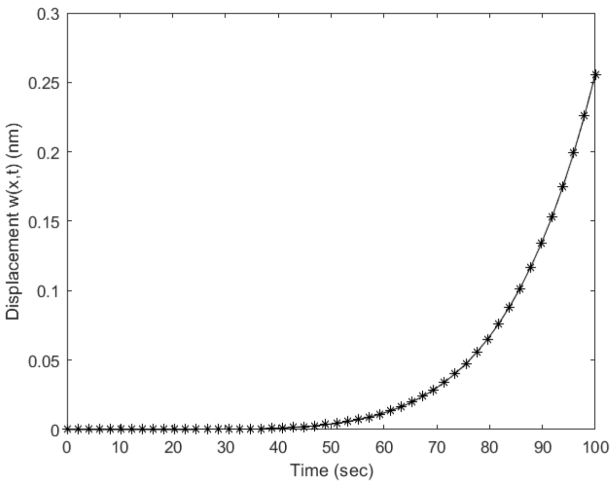

Figure 4. Response of the tube at mode 2 (n=2).

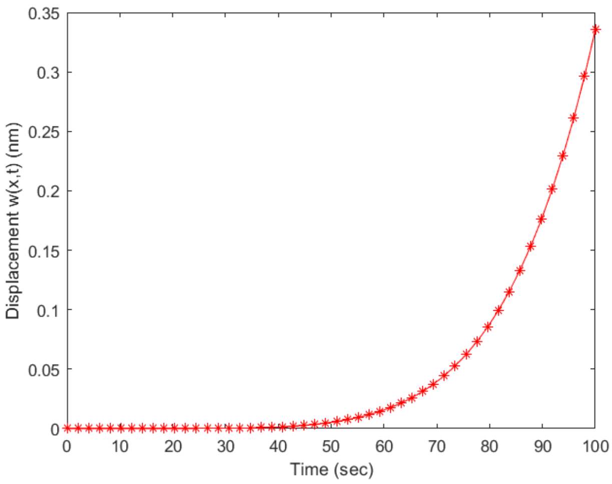

Figure 5. Response of the tube at mode 3 (n=3).

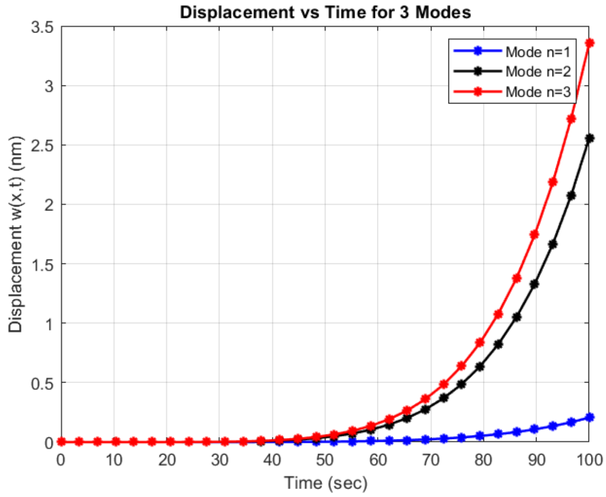

Figure 6. Relationship across all 3 modes superimposed.

Dynamic response with after-treatment technique (Figures 7-10)

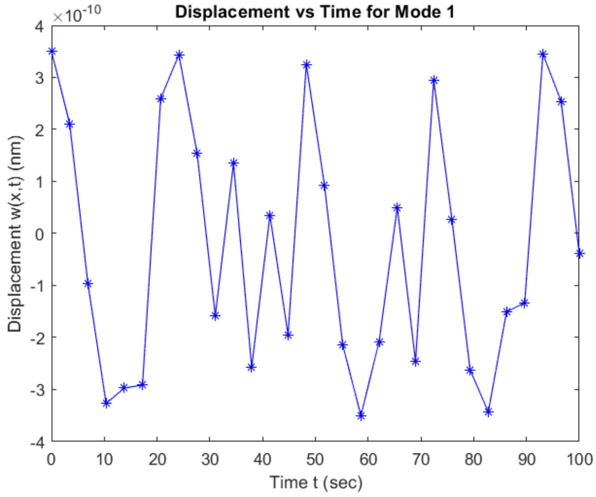

Figure 7. Midpoint deflection response of the tube at mode 1 (n=1).

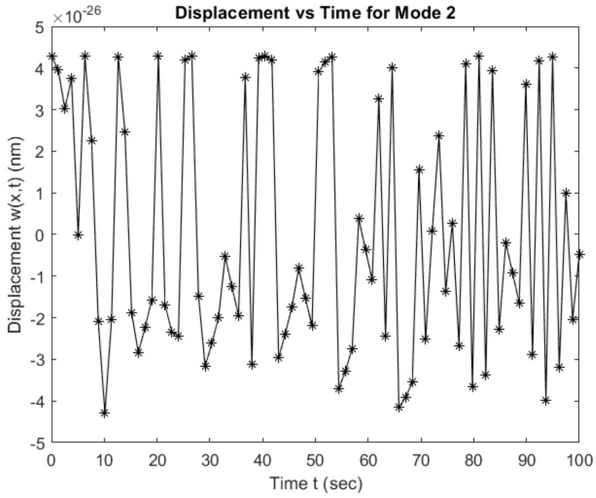

Figure 8. Midpoint deflection response of the tube at mode 2 (n=2).

https://doi.org/10.61577/jnd.2023.100006

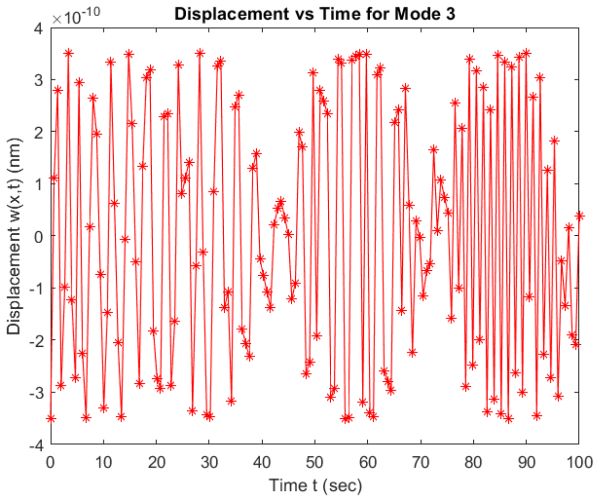

Figure 9. Midpoint deflection response of the tube at mode 3 (n=3).

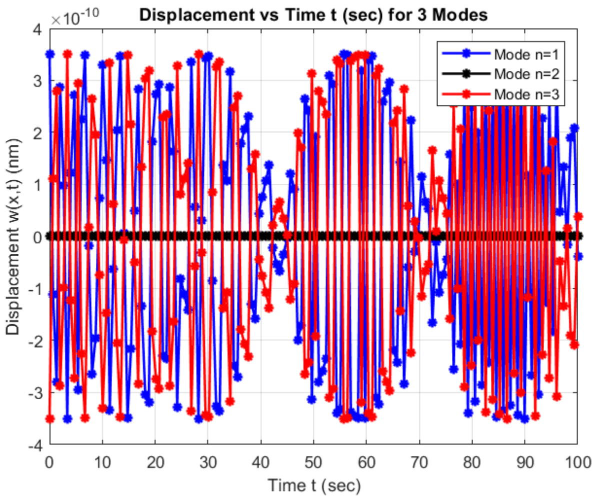

Figure 10. Midpoint deflection relationship across all 3 modes superimposed.

Steady-state analysis

This involves establishing the relationship between the mode shape function and dimensionless length of the CNT considering simple-supported systems (Figures 11-14).

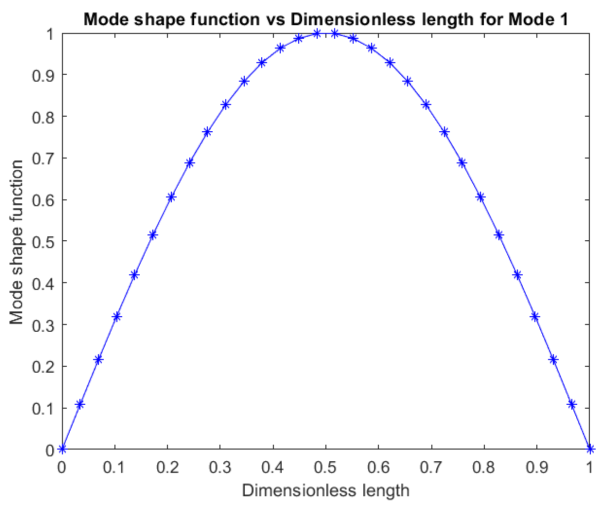

Figure 11. Mode shape function for Mode 1.

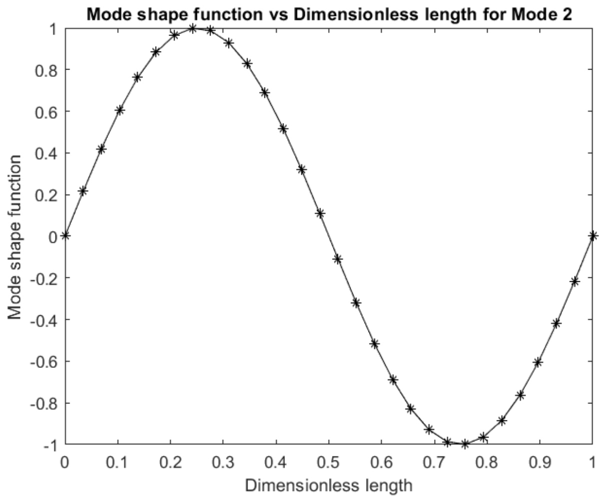

Figure 12. Mode shape function for Mode 2.

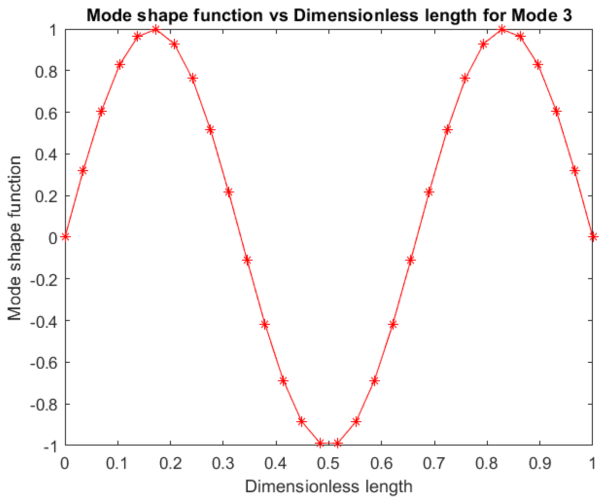

Figure 13. Mode shape function for Mode 3.

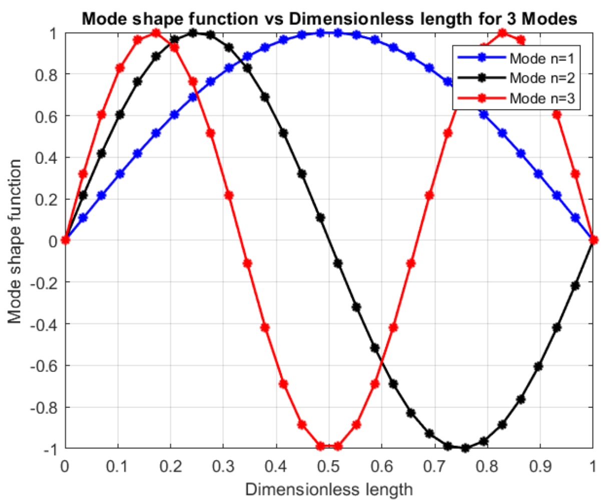

Figure 14. Mode shape function for 3 Modes.

https://doi.org/10.61577/jnd.2023.100006

RESEAPRO JOURNALS

Stability analysis

This illustrates the effects of varying frequencies in the velocity and displacement relationship. It also shows how the displacement of the CNT is influenced by the applied harmonic traversing force (Figures 15-26).

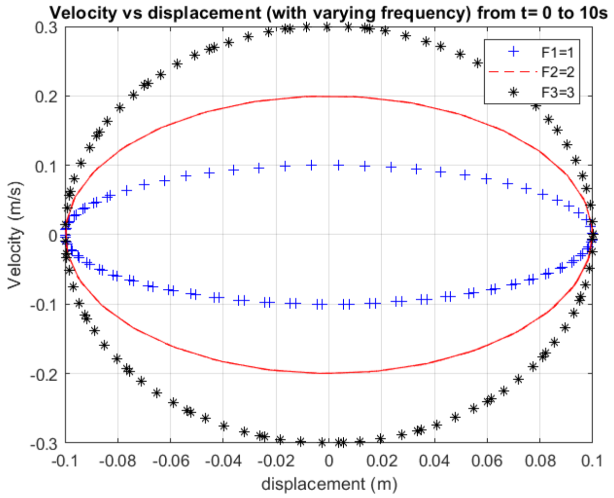

Figure 15. Phase-plane plot for stability (0 to 10s).

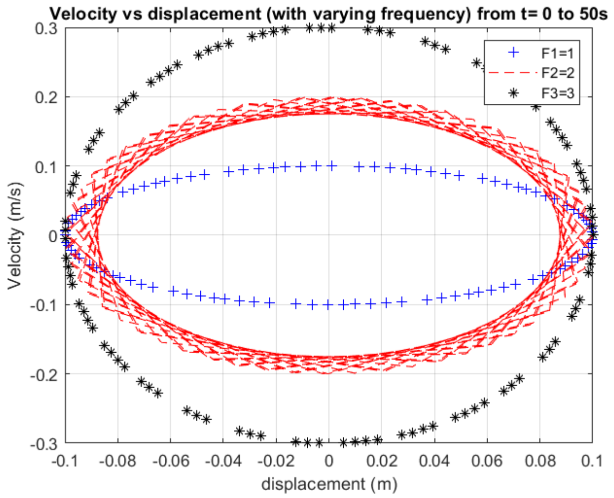

Figure 16. Phase-plane plot for stability (0 to 50s).

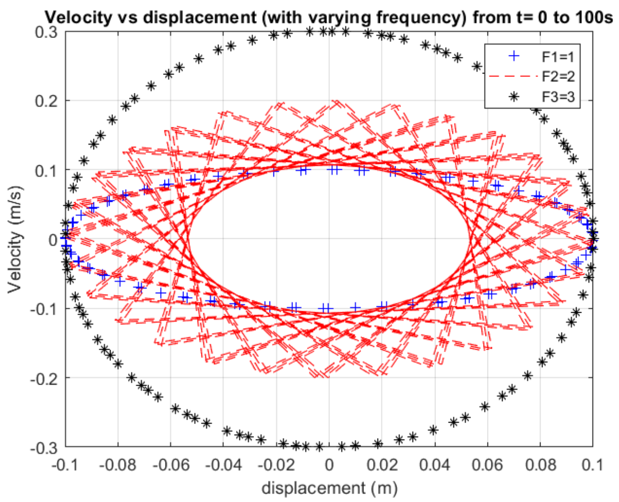

Figure 17. Phase-plane plot for stability (0 to 100s).

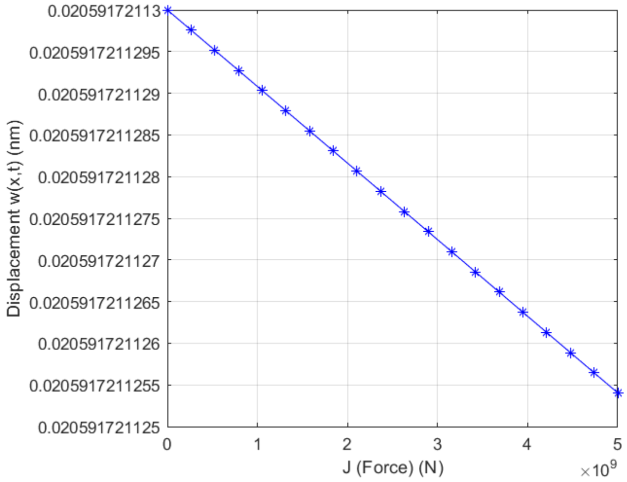

Figure 18. Stability response analysis (Force and Displacement).

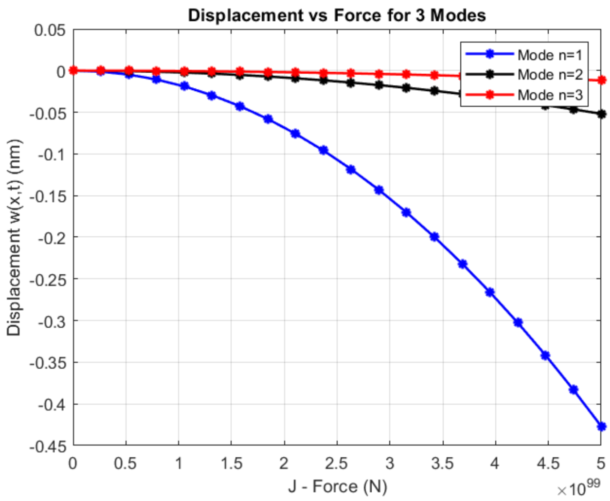

Figure 19. Stability response analysis across first 3 modes.

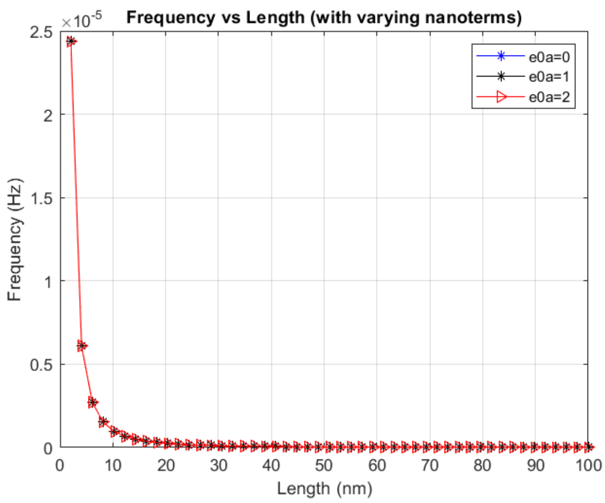

Figure 20. Stability analysis with respect to Frequency and Length.

https://doi.org/10.61577/jnd.2023.100006

RESEAPRO JOURNALS

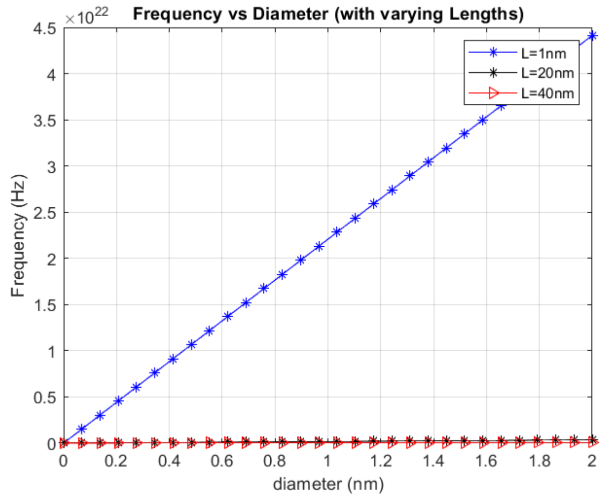

Figure 21. Effect of diameter/area on frequency and stability response.

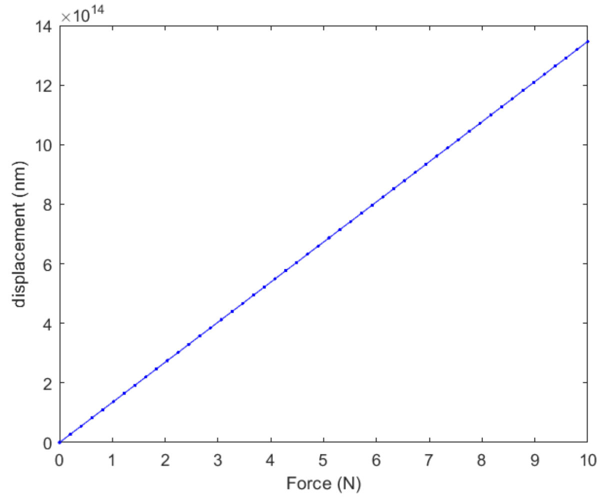

Figure 24. Effect of Force on displacement of nanotube.

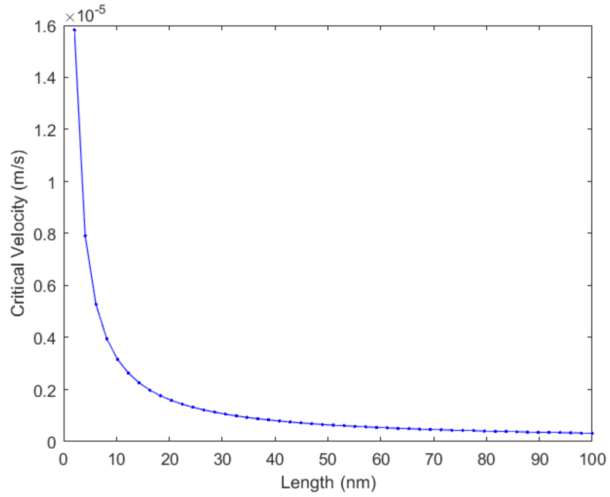

Figure 22. Plot of Critical Velocity against Length.

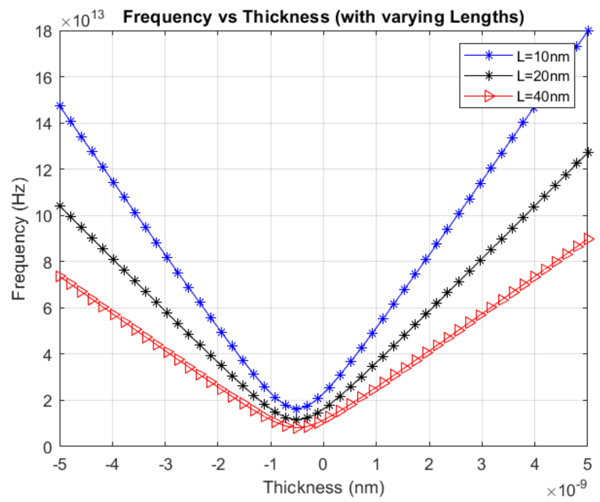

Figure 25. Effect of thickness on the frequency of nanotube.

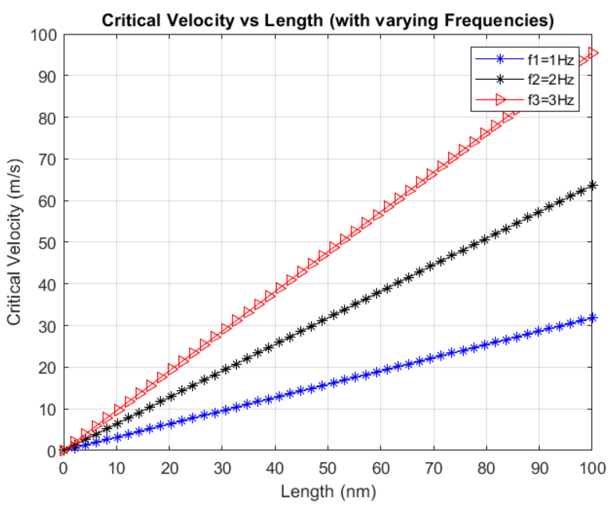

Figure 23. Effect of length and frequency on Critical velocity.

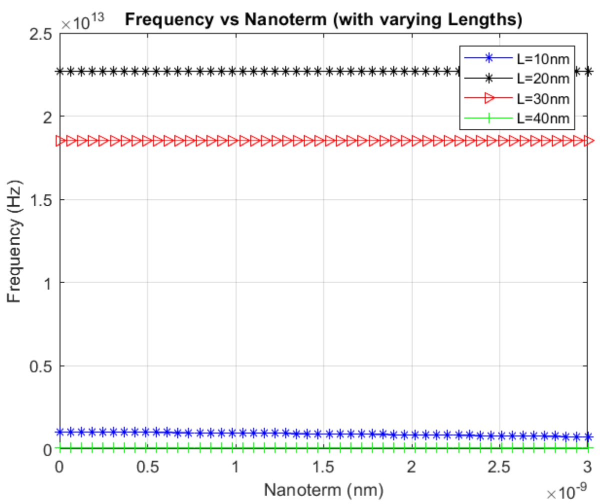

Figure 26. Effect of the nano-term on the frequency of nanotube.

https://doi.org/10.61577/jnd.2023.100006

RESEAPRO JOURNALS

Discussion of result

Figures 3-6 depict the effect of mode number on the dynamic response of the nanotube without the consideration of After-treatment techniques. The simulated solution diverges as the period of vibration increases. This is consequent upon the series solution obtained from DTM which requires appropriate treatment before usage. Meanwhile, Figures 7-10 illustrate impact of mode number on the dynamic response of the nanotube with the consideration of After-treatment technique. The coupling of After-treatment technique with the established solution helps generate convergent solutions that are dynamic nature. Generally, an increase in mode number increases the system's vibration. The introduction of force at higher modes usually results in chaos, divergence or flutter.

Figures 11-14 show the influence of mode number on the steady state response of the nanotube under investigation. This is equivalent to the deformation phenomenon in the nanotube material under steady condition. For the purpose of understanding the deformation behaviour, the mode shape profiles at different modes are considered and presented. From the super-imposed plot in Figure 14, it is evident that increasing mode number increases the frequency of the mode shape plot for the same span of dimensionless length of the nanotube. Hence, continuous increase in this parameter especially in the presence of applied load makes the nanotube loses its stability. Figures 15-17 depict the phase plate plots of the system under harmonic force for different durations. These plots are used for qualitative stability analysis. As the harmonic force increases, the phase plane curve moves outwards and away from the nodes. This further demonstrate the instability capability of the applied load.

Figures 18-26 illustrate the effects of mode number, nonlocal term, length, resonance frequency and nanotube thickness on the quantitative stability and chaotic analysis of the nanotube. From the plots, it is evident that an increase in mode number increases system's displacement and consequently reduces the stability. The nonlocal term possesses negligible effect for a span of 10nm. However, as the length of the nanotube is increase, an increase in nonlocal term tends to reduce instability in the system. The critical velocity of the system is also observed to decrease with increasing length of nanotube. Furthermore, increasing resonance frequency (due to increase in thickness and length) and applied load also increase the critical velocity of the system.

Additionally, Tables 1-3 shows the verification of the present study with numerical forth order Runge-kutta's method (RK4). Excellent agreements were recorded when the employed scheme (DTM) in this study is compared with a numerical method in MATLAB.

Table 1. Dynamic Response Analysis (Before CAT treatment).

	n = 1			n = 2			n = 3		
t	Numerical	DTM	Residue	Numerical	DTM	Residue	Numerical	DTM	Residue
0.00	3.50E-14	3.50E-14	0.0000	3.50E-14	3.50E-14	0.0000	3.50E-14	3.50E-14	0.0000
1.00	2.06E-13	2.06E-13	0.0000	2.56E-12	2.56E-12	0.0000	3.35E-12	3.35E-12	0.0000
2.00	1.32E-11	1.32E-11	0.0000	1.64E-10	1.64E-10	0.0000	2.15E-10	2.15E-10	0.0000
3.00	1.50E-10	1.50E-10	0.0000	1.87E-09	1.87E-09	0.0000	2.45E-09	2.45E-09	0.0000
4.00	8.43E-10	8.43E-10	0.0000	1.05E-08	1.05E-08	0.0000	1.37E-08	1.37E-08	0.0000
5.00	3.22E-09	3.22E-09	0.0000	4.00E-08	4.00E-08	0.0000	5.24E-08	5.24E-08	0.0000
6.00	9.61E-09	9.61E-09	0.0000	1.19E-07	1.19E-07	0.0000	1.57E-07	1.57E-07	0.0000
7.00	2.42E-08	2.42E-08	0.0000	3.01E-07	3.01E-07	0.0000	3.95E-07	3.95E-07	0.0000
8.00	5.40E-08	5.40E-08	0.0000	6.71E-07	6.71E-07	0.0000	8.79E-07	8.79E-07	0.0000
9.00	1.09E-07	1.09E-07	0.0000	1.36E-06	1.36E-06	0.0000	1.78E-06	1.78E-06	0.0000
10.00	2.06E-07	2.06E-07	0.0000	2.56E-06	2.56E-06	0.0000	3.35E-06	3.35E-06	0.0000

Table 2. Dynamic Response Analysis (After CAT treatment).

	n = 1			n = 2			n = 3		
t	Numerical	DTM	Residue	Numerical	DTM	Residue	Numerical	DTM	Residue
0.00	3.50E-10	3.50E-10	0.0000	4.29E-26	4.29E-26	0.0000	-3.50E-10	-3.50E-10	0.0000
1.00	2.34E-10	2.34E-10	0.0000	2.87E-26	2.87E-26	0.0000	-2.34E-10	-2.34E-10	0.0000
2.00	-3.69E-11	-3.69E-11	0.0000	-4.52E-27	-4.52E-27	0.0000	3.69E-11	3.69E-11	0.0000
3.00	-3.35E-10	-3.35E-10	0.0000	-4.11E-26	-4.11E-26	0.0000	3.35E-10	3.35E-10	0.0000
4.00	-3.42E-10	-3.42E-10	0.0000	-4.19E-26	-4.19E-26	0.0000	3.42E-10	3.42E-10	0.0000
5.00	-2.65E-10	-2.65E-10	0.0000	-3.24E-26	-3.24E-26	0.0000	2.65E-10	2.65E-10	0.0000
6.00	2.93E-10	2.93E-10	0.0000	3.58E-26	3.58E-26	0.0000	-2.93E-10	-2.93E-10	0.0000
7.00	5.03E-11	5.03E-11	0.0000	6.17E-27	6.17E-27	0.0000	-5.03E-11	-5.03E-11	0.0000
8.00	3.19E-10	3.19E-10	0.0000	3.91E-26	3.91E-26	0.0000	-3.19E-10	-3.19E-10	0.0000
9.00	3.19E-10	3.19E-10	0.0000	3.91E-26	3.91E-26	0.0000	-3.19E-10	-3.19E-10	0.0000
10.00	5.09E-11	5.09E-11	0.0000	6.23E-27	6.23E-27	0.0000	-5.09E-11	-5.09E-11	0.0000

https://doi.org/10.61577/jnd.2023.100006

RESEAPRO JOURNALS

Table 3. Steady-State Analysis.

	n = 1			n = 2			n = 3		
L (nm)	Numerical	DTM	Residue	Numerical	DTM	Residue	Numerical	DTM	Residue
0.00	0.00E+00	0.00E+00	0.0000	0.00E+00	0.00E+00	0.0000	0.00E+00	0.00E+00	0.0000
0.01	3.17E-02	3.17E-02	0.0000	6.34E-02	6.34E-02	0.0000	9.51E-02	9.51E-02	0.0000
0.02	6.34E-02	6.34E-02	0.0000	1.27E-01	1.27E-01	0.0000	1.89E-01	1.89E-01	0.0000
0.03	9.51E-02	9.51E-02	0.0000	1.89E-01	1.89E-01	0.0000	2.82E-01	2.82E-01	0.0000
0.04	1.27E-01	1.27E-01	0.0000	2.51E-01	2.51E-01	0.0000	3.72E-01	3.72E-01	0.0000
0.05	1.58E-01	1.58E-01	0.0000	3.12E-01	3.12E-01	0.0000	4.58E-01	4.58E-01	0.0000
0.06	1.89E-01	1.89E-01	0.0000	3.72E-01	3.72E-01	0.0000	5.41E-01	5.41E-01	0.0000
0.07	2.20E-01	2.20E-01	0.0000	4.30E-01	4.30E-01	0.0000	6.18E-01	6.18E-01	0.0000
0.08	2.51E-01	2.51E-01	0.0000	4.86E-01	4.86E-01	0.0000	6.90E-01	6.90E-01	0.0000
0.09	2.82E-01	2.82E-01	0.0000	5.41E-01	5.41E-01	0.0000	7.56E-01	7.56E-01	0.0000
0.10	3.12E-01	3.12E-01	0.0000	5.93E-01	5.93E-01	0.0000	8.15E-01	8.15E-01	0.0000

Conclusions

The present study considered forced SWCNT's vibration within the framework of the Euler-Bernoulli beam and nonlocal elasticity models. The Galerkin's approach was used to convert the governing partial differential equation into ordinary differential equation. The converted equation was solved using DTM, and then treated using CAT. The simulations and graphical illustrations which were done using MAPLE and MATLAB software were used for parametric study. Key findings gotten from these analyses are as follows:

• Chaos in the CNT may be controlled by using the nonlocal parameter and the velocity of transverse force. Chaos occurs at low values of nonlocal term.

• Chaos in the CNT may be annulled by augmenting the magnitude of transverse force velocity.

• In this study, the magnetic, Pasternak foundation and thermal terms that were introduced yielded some significant effects in the analysis and overall behavior of the CNT. It can be concluded that chaotic motion of a CNT is largely affected by these controlling parameters.

Detecting Chaos regimes will help in selection of appropriate systems to mitigate this flutter.

Acknowledgment

The authors acknowledge the Faculty of Engineering, University of Lagos for the data provided towards the achievement of this work.

Disclosure statement

No potential conflict of interest was reported by the authors.

References

1. Eltaher MA, Mohamed N. Nonlinear stability and vibration of imperfect CNTs by doublet mechanics. Appl Math Comput. 2020;382:125311.
2. Ebrahimi R. Chaotic vibrations of carbon nanotubes subjected to a traversing force considering nonlocal elasticity theory. Proc Inst Mech Eng. 2022;236(1-2):31-40.
3. Soltani P, Farshidianfar A. Periodic solution for nonlinear vibration of a fluid-conveying carbon nanotube, based on the nonlocal continuum theory by energy balance method. Appl Math Model. 2012;36(8):3712-3724.
4. Yi X, Li B, Wang Z. Vibration analysis of fluid conveying carbon nanotubes based on nonlocal timoshenko beam theory by spectral element method. Nanomaterials. 2019;9(12):1780.
5. Ansari R, Gholami R, Ajori S. Torsional vibration analysis of carbon nanotubes based on the strain gradient theory and molecular dynamic simulations. J Vib Acoust. 2013;135(5):051016.
6. Santee DM, Gonçalves PB. Oscillations of a beam on a non-linear elastic foundation under periodic loads. Shock Vib. 2006;13:273-284.
7. Hosseini M, Sadeghi-Goughari M. Vibration and instability analysis of nanotubes conveying fluid subjected to a longitudinal magnetic field. Appl Math Model. 2016;40(4):2560-2576.
8. Yinusa AA, Sobamowo MG, Adelaja AO. Nonlinear vibration analysis of an embedded branched nanofluid-conveying carbon nanotube: Influence of downstream angle, temperature change and two dimensional external magnetic field. Nano Mater Sci. 2020;2(4):323-332.
9. Malikan M, Eremeyev VA, Sedighi HM. Buckling analysis of a non-concentric double-walled carbon nanotube. Acta Mech. 2020;231(12):5007-5020.
10. Aminikhah H, Hemmatnezhad M. Nonlinear vibrations of multiwalled carbon nanotubes under various boundary conditions. Int J Differ Equ. 2011;2011.
11. Barari A, Kaliji HD, Ghadimi M, Domairry G. Non-linear vibration of Euler-Bernoulli beams. Lat Am J Solids Struct. 2011;8:139-148.
12. Malikan M, Nguyen VB, Tornabene F. Damped forced vibration analysis of single-walled carbon nanotubes resting on viscoelastic foundation in thermal environment using nonlocal strain gradient theory. Eng Sci Technol an Int J. 2018;21(4):778-786.
13. Ahmad MZ, Alsarayreh D, Alsarayreh A, Qaralleh I. Differential transformation method (DTM) for solving SIS and SI epidemic models. Sains Malays. 2017;46(10):2007-2017.
14. Ganesh EN. Single walled and multi walled carbon nanotube structure, synthesis and applications. IJITEE. 2013;2(4):311-320.
15. Sasrimuang S, Chuchuen O, Artnaseaw A. Synthesis, characterization, and electrochemical properties of carbon nanotubes used as cathode materials for Al–air batteries from a renewable source of water hyacinth. Green Process Synth. 2020;9(1):340-348.
16. Kumar R, Deol S. Nonlocal buckling analysis of single-walled carbon nanotube using Differential Transform Method (DTM). Int J Sci Res. 2016;5(3).
17. Orynyak IV, Dubyk YR, Batura AS. Analysis of fluid-induced vibrations of long branched pipelines. Strength Mater. 2015;47:314-331.
18. Akour SN. Dynamics of nonlinear beam on elastic foundation. Proc World Congr Eng. 2010;2:1427-1433.
19. Fakhrabadi MM, Rastgoo A, Ahmadian MT. Nonlinear dynamic

https://doi.org/10.61577/jnd.2023.100006

analysis of electrostatically actuated single-walled carbon nanotubes using nonlocal elasticity. Lat Am J Solids Struct. 2015;12:1224-1240.

20. Mohammadimehr M, Saidi AR, Ghorbanpour Arani A, Arefmanesh A, Han Q. Buckling analysis of double-walled carbon nanotubes embedded in an elastic medium under axial compression using non-local Timoshenko beam theory. Proc Inst Mech Eng C. 2011;225(2):498-506.
21. Wang CM, Zhang YY, Ramesh SS, Kitipornchai S. Buckling analysis of micro-and nano-rods/tubes based on nonlocal Timoshenko beam theory. J Phys D: Appl Phys. 2006;39(17):3904.
22. Kumar D, Heinrich C, Waas AM. Buckling analysis of carbon nanotubes modeled using nonlocal continuum theories. J Appl Phys. 2008;103(7).
23. Kiani Y. Free vibration of functionally graded carbon nanotube reinforced composite plates integrated with piezoelectric layers. Comput Math Appl. 2016;72(9):2433-2449.
24. Sears A, Batra RC. Macroscopic properties of carbon nanotubes from molecular-mechanics simulations. Phys Rev B. 2004;69(23):235406.
25. Shen HS, Xiang Y. Nonlinear analysis of nanotube-reinforced composite beams resting on elastic foundations in thermal environments. Eng Struct. 2013;56:698-708.
26. Han Y, Elliott J. Molecular dynamics simulations of the elastic properties of polymer/carbon nanotube composites. Comput Mater Sci. 2007;39(2):315-323.
27. Lee HL, Chang WJ. Free transverse vibration of the fluid-conveying single-walled carbon nanotube using nonlocal elastic theory. J Appl Phys. 2008;103(2).
28. Liang F, Su Y. Stability analysis of a single-walled carbon nanotube conveying pulsating and viscous fluid with nonlocal effect. Appl Math Model. 2013;37(10-11):6821-6828.
29. Ebrahimian MR, Imam A, Najafi M. The effect of chirality on the torsion of nanotubes embedded in an elastic medium using doublet mechanics. Ind J Phys. 2020;94:31-45.
30. Eltaher MA, Mahmoud FF, Assie AE, Meletis E. Coupling effects of nonlocal and surface energy on vibration analysis of nanobeams. Appl Math Comput. 2013;224:760-774.
31. Fatahi-Vajari A, Imam A. Torsional vibration of single-walled carbon nanotubes using doublet mechanics. Z Angew Math Phys. 2016;67:1-22.
32. Sobamowo MG, Akanmu JO, Adeleye OA, Akingbade SA, Yinusa AA. Coupled effects of magnetic field, number of walls, geometric imperfection, temperature change, and boundary conditions on nonlocal nonlinear vibration of carbon nanotubes resting on elastic foundations. Forces Mech. 2021;3:100010.
33. Yinusa AA, Sobamowo MG, Adelaja AO. Thermal analysis of nanofluidic flow through multi-walled carbon nanotubes subjected to perfectly and imperfectly bonded wall conditions. Chem Thermodyn Therm Anal. 2022;5:100028.
34. Gangoli VS, Yick T, Bian F, Orbaek White A. From waste plastics to carbon nanotube audio cables. C. 2022;8(1):9.
35. Torres-Dias AC, Impellizzeri A, Picheau E, Noé L, Penicaud A, Ewels C, et al. Asymmetrical Cross-Sectional Buckling in Arc-Prepared Multiwall Carbon Nanotubes Revealed by Iodine Filling. C. 2022;8(1):10.

https://doi.org/10.61577/jnd.2023.100006